Polymerization in Frameworks

DOI: 10.1002/ange.201205618

Confined Polymerization in Porous Organic Frameworks with an Ultrahigh Surface Area**

Angiolina Comotti, Silvia Bracco, Martino Mauri, Sergio Mottadelli, Teng Ben, Shilun Qiu, and Piero Sozzani*

Porous organic polymers, a class of amorphous polymers exhibiting permanent microporosity, appear to be a resourceful area for their potential applications in gas storage, separation, and catalysis.[1] The scenario of microporous organic polymers has recently emerged as one of the most stimulating fields to achieve high-surface-area materials and large absorption capacities. Their preparation takes advantage of the increasing number of modern bond-forming methods that have opened new synthetic ways for their construction.[2] Among the most promising microporous polymers are those constructed by rigid monomers that can cross-link by coupling chemistry, yielding hypercross-linked networks with pores of uniform size.[3,4] Remarkably, polymers constituted by tetrahedral nodes covalently connected by diphenyl linkers[3] reach exceptionally high surface areas that are comparable to those of the last generation MOFs and COFs.[5] In contrast to porous crystalline materials with coordination bonds, microporous organic polymers do not usually exhibit long-range order but feature robust and fully covalent frameworks, expanding both the chemical and physical operative conditions for applications. The extraordinary chemical stability of microporous organic polymers makes them ideal for supporting chemical reactions without framework destruction or loss of porosity. However, despite the potential of such host frameworks and the expectedly large monomer uptake, polymerization within their pores has never been reported.

Herein we propose the use of a prominent ultrahigh-surface-area porous network consisting by diphenyl linkers connected by tetrahedral carbon joints (PAF1) as a host for in situ solid-state polymerization and for the fabrication of innovative nanostructured materials. Confined-state polymerization is an absolute novelty in the field of ultrahigh-surface-area porous materials ($SA_{BET} > 5000\ m^2 g^{-1}$). The diamondoid framework topology imposed by the tetrahedral building blocks provides open and interconnected pores that are prone to efficiently capture a large amount of monomer. The in situ polymerization allowed the synthesis of interpenetrated network in which the robust and structured porous framework serves as both the matrix and the reinforcement for the engendered polymer (Scheme 1). As a case study, we explored the polymerization of acrylonitrile because a feature of the resulting polymer (PAN) is that it thermally transforms into a rigid and conjugated ladder polymer,[6] thus paving the way to the development of materials with innovative functional properties.

Polymerization in nanospaces has been studied extensively, and has recently attracted considerable interest as a novel route to functional materials.[7] It can be considered a powerful method for controlling polymer architecture over various hierarchical levels, such as microstructure, morphol-

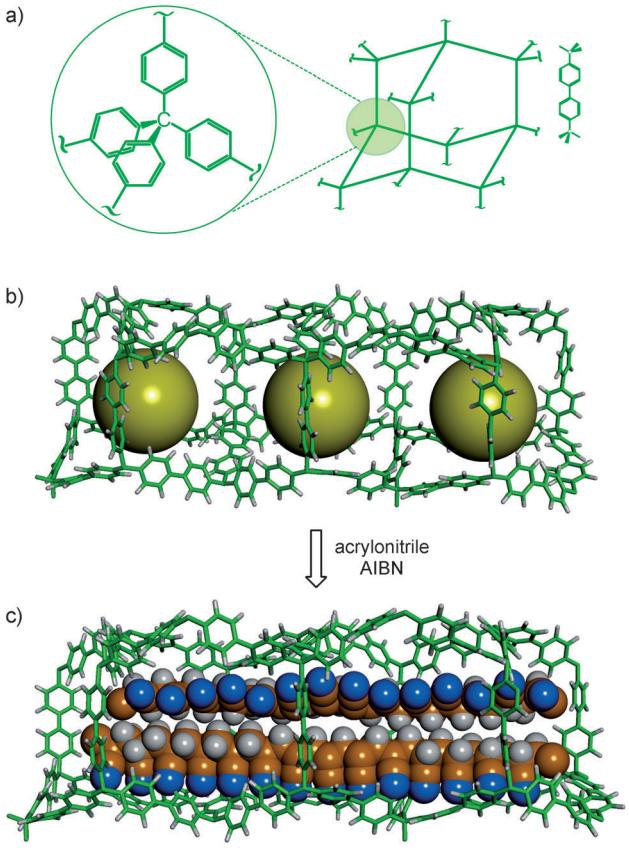

Scheme 1. Porous aromatic framework PAF1. a) Structural building blocks; b) a nanochannel of about 14 Å diameter (the yellow spheres depict the space available); c) the polymer formed by in situ polymerization of acrylonitrile within the pores (C brown, H gray, N blue).

[*] Prof. A. Comotti, Dr. S. Bracco, M. Mauri, S. Mottadelli, Prof. P. Sozzani
Department of Materials Science, University of Milano Bicocca
Via R. Cozzi 53, Milano (Italy)
E-mail: angiolina.comotti@mater.unimib.it
Prof. T. Ben, Prof. S. Qiu
State Key Laboratory of Inorganic Synthesis and Preparative Chemistry, Jilin University
Changchun (China)

[**] This work was supported by Regione Lombardia, Fondazione Cariplo, and MIUR. We thank Dr. A. Cattaneo for the support in the NMR work.

Supporting information for this article is available on the WWW under http://dx.doi.org/10.1002/anie.201205618.

ogy, and nano- and micro-object generation, thus accessing properties that are distinctly different from those of the corresponding bulk phases.[8] Intense activity is presently aimed at developing well-designed synthetic routes for the fabrication of nanostructured materials, nanocomposites, and interpenetrating polymers.[9] In this context, the porous aromatic frameworks (PAFs) could offer an unexplored opportunity to polymerize into materials with far more extended interfaces than commonly realized.

The N_2 adsorption isotherm at 77 K of the porous network PAF1 exhibits an extremely high surface area of 5340 $m^2 g^{-1}$ and 7164 $m^2 g^{-1}$ (BET and Langmuir analyses, respectively), a challenging pore volume capacity of 2.6 $cm^3 g^{-1}$, and a homogeneous pore size distribution centered at 14 Å as calculated by NLDFT analysis (Figure 1). The porous network was soaked with acrylonitrile monomer containing the radical initiator 2,2′-azobisisobutyronitrile and, after removal of the monomer excess, the powder was heated at 100 °C for 4 h under inert atmosphere to accomplish the polymerization. In the final nanostructured PAF1-PAN, we observed a drastic reduction of both surface area and pore volume to 356 $m^2 g^{-1}$ (BET) and a 0.16 $cm^3 g^{-1}$, respectively, owing to the polymer occupying the pores. SEM analysis showed that no excess polymer was present on the external surfaces of the circa 480 nm nanoparticles (Supporting Information).

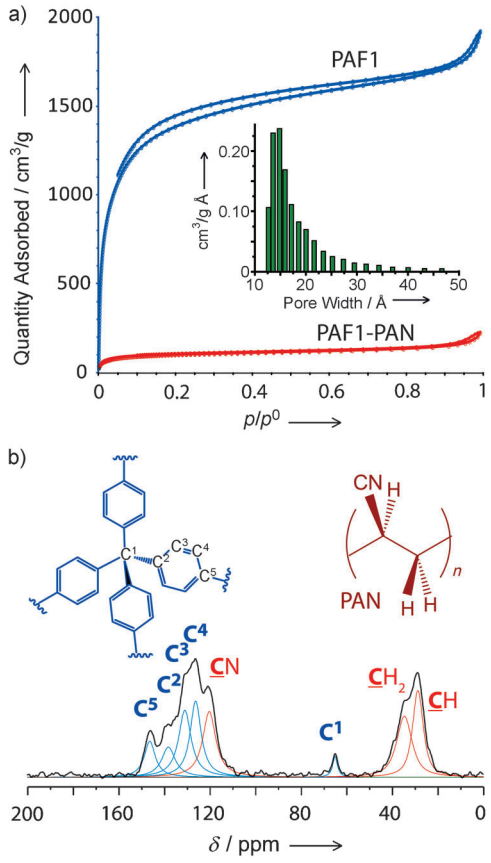

Figure 1. a) N_2 adsorption isotherms of PAF1-PAN and pure PAF1 at 77 K. The inset shows the pore size distribution. b) Quantitative 1D ^{13}C MAS NMR (recycle delay of 100 s, 15 kHz spinning speed) of PAF1-PAN with deconvoluted signals of PAN (red) and PAF1 (blue).

Thermogravimetric analysis demonstrated that a remarkable amount of poly(acrylonitrile) is found in the nanocomposite (Supporting Information). The pristine empty PAF1 showed, under nitrogen atmosphere, a weight loss of about 21 % at a temperature as high as 550 °C, whilst PAF1-PAN displayed an overall decrease of 65 %. During the heating process, the intramolecular cyclization, aromatization, and carbonization of PAN generated gas evolution, which consisted of a hydrogen and nitrogen-rich mixture. Considering these reactions, the amount of poly(acrylonitrile) in the nanocomposite is calculated to be 55 % by weight.

Independent information concerning the composition of the nanostructured material was obtained from a quantitative ^{13}C MAS NMR spectrum. It highlights the formation of the polymer and the absence of residual monomer: the characteristic signals of poly(acrylonitrile) and host matrix were observed exclusively (Figure 1 b). From the integrals of the peaks, the polymer content was estimated to be 58 % by weight. The content of included polymer in the network is exceptionally high compared to that of confined polymerization in microporous materials,[7a] and corresponds to a theoretical pore-filling of at least 80 % v/v of the pore volume based on bulk density of PAN and the total free volume of PAF. The guest/host ratio is 8.4:1; that is, one monomeric unit of the guest per each face of host aromatic ring. Once extracted from the matrix, PAN showed a molecular mass as high as 80 kDa.

Given the absence of crystallinity in PAF1, as in porous organic polymers in general, XRD cannot be of help to elucidate the structure of PAF1-PAN. Fast magic-angle-spinning 2D ^1H–^{13}C HETCOR NMR spectra (Figure 2), performed under Lee–Goldburg homonuclear decoupling, resulted in a unique observation of intermolecular relationships across the extremely extended interfaces. The 2D spectra collected at a contact time of 0.1 ms emphasized only the correlations of the hydrogen and carbon nuclei sitting at covalent bond distances (Figure 2 a). In contrast, in the 2D spectrum with a contact time of 0.5 ms, new cross-peaks between the host aromatic hydrogen atoms ($\delta_H = 7.0$ ppm) and PAN carbon atoms (δ_{CH} and δ_{CH_2} at 28.7 and 34.6 ppm) clearly appeared. This is a rare case wherein an intermolecular cross-peak is detected at such a short contact time, demonstrating the close proximity, at the molecular level, of the poly(acrylonitrile) chains and the aromatic moieties lining the host pores. At longer contact times, all mutual cross-peaks between host and guest increase progressively owing to the strong dipole–dipole nuclear intermolecular interactions. The intense through-space communication at the host–PAN interfaces reveals the massive interaction, the intimate relationship between host and guest moieties, and the extensively interdigitated nanophases.

Monodimensional ^1H *w*PMLG MAS NMR (Figure 2 f), indicates that signals for incorporated PAN CH and CH_2 groups appear upfield ($\delta_H = 2.2$ and 1.7 ppm, respectively) compared to the signals of neat PAN ($\delta_H = 3.1$ and 2.3 ppm for CH and CH_2 species) owing to the magnetic-susceptibility effect of the aromatic host rings.[10] Indeed, the two components are tightly interwoven and the linear chains are threaded through the continuous network of the hypercross-

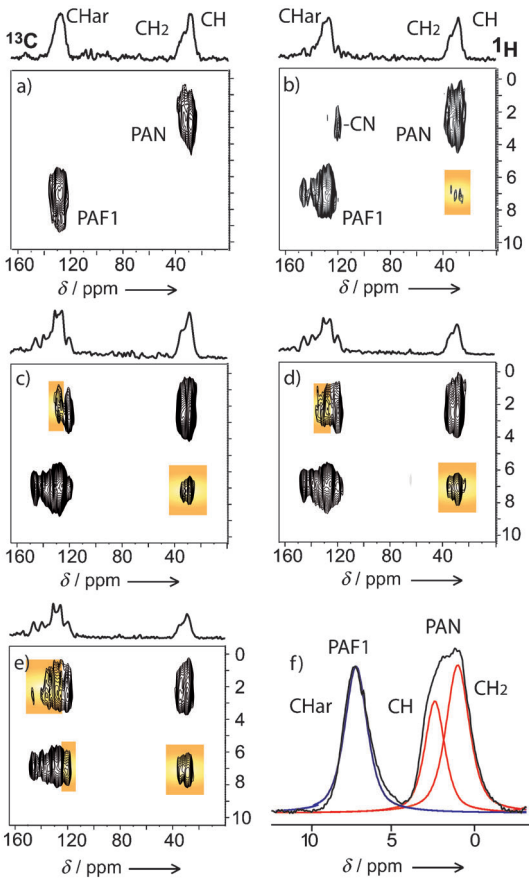

Figure 2. 2D ^{1}H–^{13}C HETCOR phase-modulated Lee–Goldburg (PMLG) 15 kHz MAS NMR of PAF1-PAN at contact times of: a) 0.1, b) 0.5, c) 1, d) 2, and e) 5 ms. Intermolecular correlations between PAF1 and PAN are shown in orange, with ^{13}C projections given above. f) ^{1}H *w*PMLG MAS NMR of PAF1-PAN at 14 T.

linked polymer. Although the two polymers would have poor compatibility and diverging physical properties, the achievement of such an intimate integration, at the molecular level, was realized by exploiting the enormous surface area of the host on which the monomer could be adsorbed. The balanced composition of the two polymers (about 50% by weight) and the open windows connecting the cages generate an intriguing nanostructure wherein the respective roles of host and guest might be ideally exchanged. In fact, poly(acrylonitrile) can be thought of as the matrix which incorporates a 3D aromatic network as a reinforcement grid.

Polymerizations with excess monomer were performed to yield nanocomposite materials containing PAF1-PAN nanoparticles dispersed in a polymeric continuous phase. The most remarkable nanocomposite product consisted of 93% PAN by weight (PAF1-*exc*PAN), as determined by DSC, FTIR, and NMR spectroscopy (Supporting Information). 2D ^{1}H–^{13}C HETCOR solid-state NMR spectra showed, in addition to intense signals of the polymeric continuous phase, host–guest intermolecular correlations brought about by the intimacy of PAF1 with PAN within the nanoparticles, thus demonstrating that PAN was both polymerized inside PAF1 nanoparticles and in the interparticle space. The aromatic rings of PAF1, individually exposed to the polymer at the extended interfaces, induce multiple and favorable CH···π interactions with the polymer chains, as demonstrated by the close-contact interactions between PAN aliphatic hydrogen atoms and aromatic carbon atoms. Thus, the interactions of PAN chains with the aromatic groups at the interface ensure that the continuous phase is firmly anchored to the porous network. It is worth noting that no reactants are needed to promote polymer–particle microadhesion, as frequently proven necessary with non-porous nanoparticles.[11] This example showed the possibility of constructing, in a single polymerization step, a hierarchical architecture wherein the first-level nanocomposite, that is, PAN confined in porous PAF1 nanoparticles, is embedded in a polymer continuous phase forming the second-level nanocomposite.

Moreover, the PAF1 matrix can be envisaged as a support for thermally activated chemical reactions. In fact, in the PAF1-PAN compound thermal transformations of PAN within the framework produced an innovative material composed by two rigid structures: a stiff-chain polymer and a 3D framework. The first stage of the process involved exothermal cyclization by the reaction of adjacent nitrile groups along the polymer chain, which evolves into a polyconjugated ladder-structured polymer, containing C=N and C=C unsaturations (Figure 3a). The DSC run at 10 °C min^{-1} displayed an exotherm at 290 °C that is due to the intramolecular polymerization of nitrile groups. Notably, the observed temperature of the phenomenon is shifted 20 °C higher than in the reference bulk PAN (Figure 3b) because the kinetics of the transformation is slowed down when the polymer chains are strictly interwoven with the aromatic framework, as shown by scans at variable heating rates (Supporting Information). In other words, a regulatory mechanism applies to the confined polymer chains, thus confirming the extensive interaction of the reacting polymer chains with the inert host 3D network. The comparison between cyclisation enthalpy of PAF1-PAN (about 500 J g^{-1} as normalized on PAN) and that of neat PAN (550 J g^{-1}) suggested that most PAN is transformed within the network to the product. Following the transformation by ^{13}C MAS NMR, we detected chemical shifts diagnostic of C=N and C=C groups; these new groups occur at the expense of the nitrile CN and aliphatic groups. The new resonances were also recognized in the ladder-structured polymer as obtained from bulk PAN, demonstrating that the structural transformation of the PAN in PAF1 matrix follows the same reaction pathway (Supporting Information). Cross-peaks in 2D ^{1}H-^{13}C HETCOR MAS NMR of the PAF1-PAN compounds, heated to 350 °C for 30 min and for 4 h, indicated a short-distance communication between the ladder polymer formed in situ from PAN and the framework, thus highlighting, after curing, the persistence of the intimate entanglement among the components within the novel semi-interpenetrated material (Supporting Information).

FTIR spectroscopy could also confirm the cyclization reaction of PAN encaged in the PAF1 network (Figure 3c). After heating the sample under an inert atmosphere from 270 °C to 350 °C, the characteristic band at 2245 cm^{-1} of CN stretching disappeared and new bands became visible. The presence of an intense signal at 1611 cm^{-1} that is due to

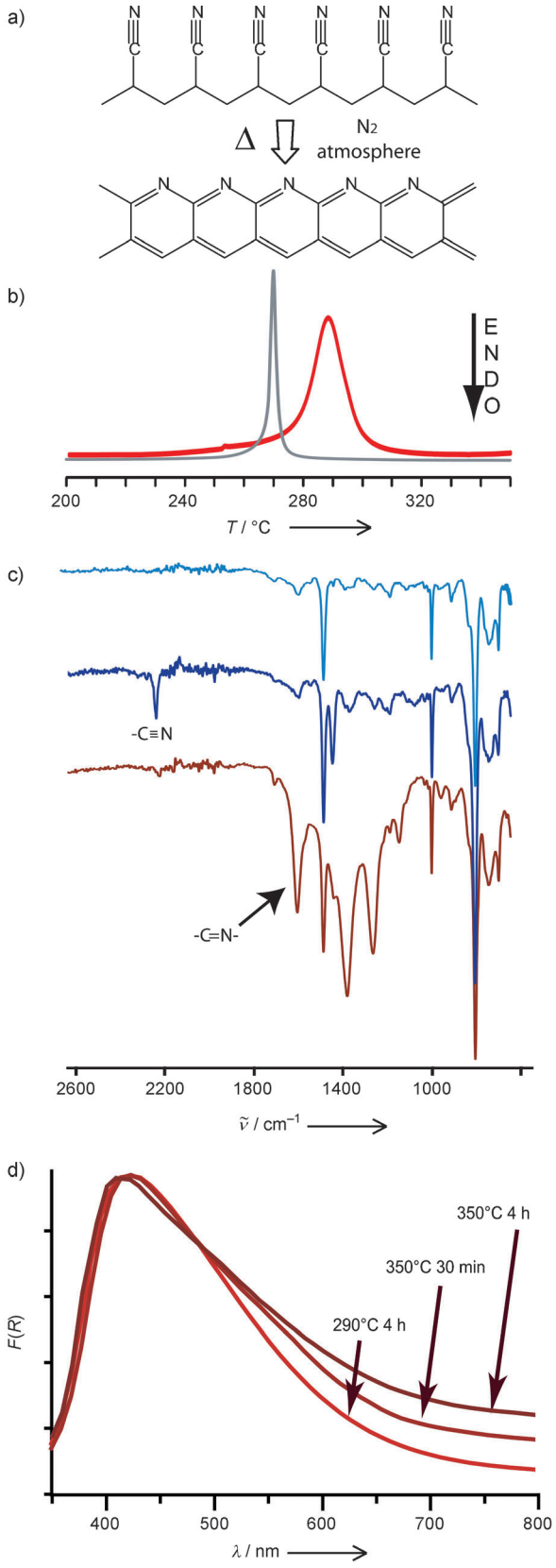

Figure 3. a) Thermal transformation of PAN into the ladder polymer. b) DSC of PAF1-PAN (red) and pure PAN (gray). c) FTIR spectra of porous PAF1 (light blue), PAF1-PAN (blue), and PAF1-PAN (red) heated to 350°C. d) Vis/NIR diffuse reflectance spectra of PAF1-PAN nanocomposites heated at different temperatures and curing times. The Kubelka–Munk absorption coefficient ($F = K/S$) is shown.

stretching of -C=N- is a clear demonstration of the occurred intramolecular cyclization. Notably, the infrared bands of the host matrix do not change during the thermal treatment, indicating that the PAF1 network does not undergo any significant chemical modification up to 350°C.

The electronic conjugation of the newly-formed double bonds along the ladder polymer structure conferred, progressively, a bright yellow, orange and, finally, red-brown color to the material.[6] The progress of the reaction and the bathochromic color shift can be regulated by temperature/time conditions. Optical absorption of the cured nanocomposites in the visible and near-infrared spectra (from 300 to 800 nm) allowed the monitoring, step-by-step, of the reaction progress, and highlighted the feasibility of the fine-modulation of the structure by programming the curing time and temperature (Figure 3d). In fact, on increasing the curing temperature, the absorption profile intensifies at wavelengths from 500 nm to 800 nm, which correspond to energy gaps from 2.5 to 1.5 eV. The energy gaps fall in the interval described for polyconjugated molecular systems with semiconducting properties. Thus, in the semi-interpenetrated network we could selectively transform one of the two components, and enhance both the electronic properties and the backbone rigidity of a ladder polymer interwoven with the aromatic scaffold, thus opening the way to the construction of unique organic semiconductors in a robust covalent framework.[12] This is an unusual method to fabricate a 3D network of two rigid and nonmeltable polymers that are not expected to be blended effectively otherwise.

The present work provided the first evidence of the feasibility of polymerization in ultrahigh-surface-area nanoporous materials. Solid-state 2D NMR and complementary techniques have been effective in describing the intimacy of the nanophases, polymer confinement, and pore filling. Through in-depth characterization it was possible to attain a model in which poly(acrylonitrile) chains interact with the connectors of the continuous three-dimensional network of the porous host, resulting in a material that consist of two distinct, very intimately entangled components. The polymer therein engendered can be further transformed in situ at high temperatures thanks to the extremely high thermal robustness of the aromatic framework, which assists the metamorphosis of the linear polymer without degradation of its architecture.

The rapid developments in porous polymer networks, with increasingly higher pore capacity and surface areas, can be expected to result in the generation of nanocomposites with fine-tuned polymer–polymer interactions and a variety of functions, such as the absorption/emission of light. Moreover, the modulation of the steric environments and chemical functions of linkers will provide molecular-level shape selectivity and chemical reactivity to construct a versatile platform for the formation of new interpenetrated nanostructured materials with predesigned properties.

Received: July 15, 2012
Published online: September 5, 2012

Keywords: host–guest systems · ladder polymers · microporous materials · nanostructures · polymerization

[1] a) N. B. Mckewon, P. M. Budd, *Macromolecules* **2010**, *43*, 516 – 521; b) J. R. Holst, A. I. Cooper, *Adv. Mater.* **2010**, *22*, 5212 – 5216; c) N. B. McKeown, P. M. Budd, *Chem. Soc. Rev.* **2006**, *35*, 675 – 683; d) K. Kaur, J. T. Hupp, S. T. Nguyen, *ACS Catal.* **2011**, *1*, 819 – 835; e) T. Ben, C. Pei, D. Zhang, J. Xu, F. Deng, X. Jing, S. Qiu, *Energy Environ. Sci.* **2011**, *4*, 3991 – 3999; f) A. Thomas, *Angew. Chem.* **2010**, *122*, 8506 – 8523; *Angew. Chem. Int. Ed.* **2010**, *49*, 8328 – 8344.

[2] a) R. Chinchilla, C. Najera, *Chem. Rev.* **2007**, *107*, 874 – 922; b) N. Miyaura, A. Suzuki, *Chem. Rev.* **1995**, *95*, 2457 – 2483; c) M. Meldal, C. W. Tornøe, *Chem. Rev.* **2008**, *108*, 2952 – 3015.

[3] a) T. Ben, H. Ren, S. Q. Ma, D. P. Cao, J. H. Lan, X. F. Jing, W. C. Wang, J. Xu, F. Deng, J. M. Simmnos, S. L. Qiu, G. S. Zhu, *Angew. Chem.* **2009**, *121*, 9621 – 9624; *Angew. Chem. Int. Ed.* **2009**, *48*, 9457 – 9460; b) D. Yuan, W. Lu, D. Zhao, H. C. Zhou, *Adv. Mater.* **2011**, *23*, 3723 – 3725; c) W. G. Lu, D. Q. Yuan, D. Zhao, C. I. Schilling, O. Plietzsch, T. Muller, S. Brase, J. Guenther, J. Blumel, R. Krishna, Z. Li, H. C. Zhou, *Chem. Mater.* **2010**, *22*, 5964 – 5972.

[4] a) C. D. Wood, B. Tan, A. Trewin, F. Su, M. J. Rosseinsky, D. Bradshaw, Y. Sun, L. Zhou, A. I. Cooper, *Adv. Mater.* **2008**, *20*, 1916 – 1923; b) H. Ren, T. Ben, E. S. Wang, X. F. Jing, M. Xue, B. B. Liu, Y. Cui, S. L. Qiu, G. S. Zhu, *Chem. Commun.* **2010**, *46*, 291 – 293; c) H. Ren, T. Ben, F. Sun, M. Guo, X. Jing, H. Ma, K. Cai, S. Qiu, G. Zhu, *J. Mater. Chem.* **2011**, *21*, 10348 – 10353; d) P. Kuhn, M. Antonietti, A. Thomas, *Angew. Chem.* **2008**, *120*, 3499 – 3502; *Angew. Chem. Int. Ed.* **2008**, *47*, 3450 – 3453; e) T. Ben, K. Shi, Y. Cui, C. Pei, Y. Zuo, H. Guo, D. Zhang, J. Xu, F. Deng, Z. Tian, S. Qiu, *J. Mater. Chem.* **2011**, *21*, 18208 – 18214.

[5] a) H. Furukawa, N. Ko, Y. B. Go, N. Aratani, S. B. Choi, E. Choi, A. Ö. Yazaydin, R. Q. Snurr, M. O 'Keeffe, J. Kim, O. M. Yaghi, *Science* **2010**, 329, 424 – 428; b) O. K. Farha, A. O. Yazaydin, I. Eryazici, C. D. Malliakas, B. G. Hauser, M. G. Kanatzidis, S. T. Nguyen, R. Q. Snurr, J. T. Hupp, *Nat. Chem.* **2010**, *2*, 944 – 948; c) H. M. El-Kaderi, J. R. Hunt, J. L. Mendoza-Cortez, A. P. Côté, R. E. Taylor, M. O'Keefe, O. M. Yaghi, *Science* **2007**, *316*, 268 – 272.

[6] a) M. S. A. Rahaman, A. F. Ismail, A. A. Mustafa, *Polym. Degrad. Stab.* **2007**, *92*, 1421 – 1432; b) O. Ruzimuradov, G. Rajan, J. Mark, *Macromol. Symp.* **2006**, *245 – 246*, 322 – 324.

[7] a) T. Uemura, N. Yanai, S. Kitagawa, *Chem. Soc. Rev.* **2009**, *38*, 1228 – 1236; b) T. Uemura, S. Horike, K. Kitagawa, M. Mizuno, K. Endo, S. Bracco, A. Comotti, P. Sozzani, M. Nagaoka, S. Kitagawa, *J. Am. Chem. Soc.* **2008**, *130*, 6781 – 6788; c) K. Kageyama, J.-I. Tamazawa, T. Aida, *Science* **1999**, *285*, 2113 – 2115; d) C. G. Wu, T. Bein, *Science* **1994**, *266*, 1013 – 1015; e) P. Sozzani, S. Bracco, A. Comotti, R. Simonutti, *Adv. Polym. Sci.* **2005**, *181*, 153 – 177; f) M. Farina, G. Di Silvestro, P. Sozzani in *Comprehensive Supramolecular Chemistry*, *Vol. 6* (Ed.: J.-M. Lehn), Pergamon, Oxford, **1996**, pp. 371 – 398; g) K. Tajima, T. Aida, *Chem. Commun.* **2000**, 2399 – 2412; h) Y. Lu, Y. Yang, A. Sellinger, M. Lu, J. Huang, H. Fan, R. Haddad, G. Lopez, A. R. Burns, D. Y. Sasaki, J. Shelnutt, C. J. Brinker, *Nature* **2001**, *410*, 913 – 917; i) M. Miyata, K. Sada in *Comprehensive Supramolecular Chemistry*, *Vol. 6* (Ed.: J.-M. Lehn), Pergamon, Oxford, **1996**, pp. 147 – 176; j) F. C. Schilling, P. Sozzani, F. A. Bovey, *Macromolecules* **1991**, *24*, 4369 – 4375.

[8] a) B. H. Jones, T. P. Lodge, *ACS Nano* **2011**, *5*, 8914 – 8927; b) P. Sozzani, S. Bracco, A. Comotti, R. Simonutti, P. Valsesia, Y. Sakamoto, O. Terasaki, *Nat. Mater.* **2006**, *5*, 545 – 551; c) N. Yanai, T. Uemura, M. Ohba, Y. Kadowaki, M. Maesato, M. Takenaka, S. Nishitsuji, H. Hasegawa, S. Kitagawa, *Angew. Chem.* **2008**, *120*, 10031 – 10034; *Angew. Chem. Int. Ed.* **2008**, *47*, 9883 – 9886; d) M. Choi, R. Ryoo, *Nat. Mater.* **2003**, *2*, 473 – 476; e) S. Kazuki, T. Masayuki, F. Norifumi, M. Numata, S. Shinkai, *Chem. Soc. Rev.* **2007**, *36*, 415 – 435; f) S. A. Johnson, P. J. Ollivier, T. E. Mallouk, *Science* **1999**, *283*, 963 – 965.

[9] a) P. Podsiadlo, A. K. Kaushik, E. M. Arruda, A. M. Waas, B. S. Shim, J. Xu, H. Nandivada, B. G. Pumplin, J. Lahann, A. Ramamoorthy, N. A. Kotov, *Science* **2007**, *318*, 80 – 83; b) A. Seema, A. Kelarakis, L. Estevez, E. P. Giannelis, *Small* **2010**, *6*, 205 – 209; c) M. A. Snyder, M. Tsapatsis, *Angew. Chem.* **2007**, *119*, 7704 – 7717; *Angew. Chem. Int. Ed.* **2007**, *46*, 7560 – 7573; d) H. Peng, X. Sun, F. Cai, X. Chen, Y. Zhu, G. Liao, D. Chen, Q. Li, Y. Lu, Y. Zhu, Q. Jia, *Nat. Nanotechnol.* **2009**, *4*, 738 – 741; e) Y. Yang et al., *J. Am. Chem. Soc.* **2003**, *125*, 1269 – 1277 (see the Supporting Information); f) S. Spange, S. Grund, *Adv. Mater.* **2009**, *21*, 2111 – 2116; g) Z.-M. Wang, W. Wang, N. Coombs, N. Soheilnia, G. A. Ozin, *ACS Nano* **2010**, *4*, 7437 – 7450.

[10] a) S. Bracco, A. Comotti, L. Ferretti, P. Sozzani, *J. Am. Chem. Soc.* **2011**, *133*, 8982 – 8994; b) S. Waugh, R. W. Fessenden, *J. Am. Chem. Soc.* **1957**, *79*, 846 – 849; c) P. v. R. Schleyer, C. Maerker, A. Dransfeld, H. Jiao, N. J. R. Van Eikema Hommes, *J. Am. Chem. Soc.* **1996**, *118*, 6317 – 6318; d) P. Sozzani, S. Bracco, A. Comotti, R. Simonutti, *Angew. Chem.* **2004**, *116*, 2852 – 2857; *Angew. Chem. Int. Ed.* **2004**, *43*, 2792 – 2797.

[11] R. Simonutti, A. Comotti, P. Sozzani, F. Negroni, *Chem. Mater.* **1999**, *11*, 822 – 828.

[12] T.-C. Chung, Y. Schlesinger, S. Etemad, A. G. Macdiarmid, A. J. Heeger, *J. Polym. Sci. Polym. Phys.* **1984**, *22*, 1239 – 1246.

